



Spatial coherence of the longitudinal turbulence component

Larsen, Gunner Chr.; Hansen, Kurt Schaldemose

Published in:
Proceedings of EWEC 2003

Publication date:
2003

Document Version
Peer reviewed version

[Link back to DTU Orbit](#)

Citation (APA):
Larsen, G. C., & Hansen, K. S. (2003). Spatial coherence of the longitudinal turbulence component. In *Proceedings of EWEC 2003* (Vol. CD-ROM. CD 2). European Wind Energy Association (EWEA).

General rights

Copyright and moral rights for the publications made accessible in the public portal are retained by the authors and/or other copyright owners and it is a condition of accessing publications that users recognise and abide by the legal requirements associated with these rights.

- Users may download and print one copy of any publication from the public portal for the purpose of private study or research.
- You may not further distribute the material or use it for any profit-making activity or commercial gain
- You may freely distribute the URL identifying the publication in the public portal

If you believe that this document breaches copyright please contact us providing details, and we will remove access to the work immediately and investigate your claim.

SPATIAL COHERENCE OF THE LONGITUDINAL TURBULENCE COMPONENT

Gunner Chr. Larsen¹ and Kurt S. Hansen²

¹ Risø National Laboratories, Wind Energy Department, P.O. Box 49, DK-4000 Roskilde; E-mail: gunner.larsen@risoe.dk

² Department of Mechanical Engineering, Technical University of Denmark, DK-2800 Lyngby; E-mail: ksh@mek.dtu.dk

ABSTRACT: The design fatigue loading of wind turbine structures is traditionally determined from aeroelastic simulations, where a structural dynamic model is exposed to suitable synthetic turbulence wind fields. The wind fields are usually generated according to the recommendations given in the IEC 61400-1 standard, in which the turbulence is described combining the Kaimal spectrum with an exponential coherence model or, alternatively, by the Mann uniform shear spectral tensor. Recent investigations have shown that significant differences in simulated wind turbine tower fatigue loading may occur using the two suggested turbulence models. The differences in load predictions have been identified mainly to differences in the descriptions of the spatial coherence in the two turbulence models.

In order to calibrate the coherence descriptions given in the IEC 61400-1 standard, a substantial amount of full scale wind field data, extracted from "Database on Wind Characteristics" (<http://www.winddata.com/>), have been analysed. The analysis is restricted to spatial coherence of the longitudinal turbulence component, but both vertical and horizontal spatial separations have been investigated. Terrain- and atmospheric stability classifications have been merged into a classification according to the turbulence integral length scale. The measured coherences are thus parameterised in terms of turbulence integral length scale, measuring heights, (vertical/horizontal) spatial spacing, frequency and reduced frequency. Finally, a revised expression for the spatial coherence, associated with vertical separation, is compared with the measured coherences as well as with coherence predictions from the IEC 61400-1 standard as well as from the Mann model, and recommendations arising from this comparison are given.

Keywords: Coherence Models, Design Code, Turbulence, Turbulence Statistics, Spatial Coherence, Wind Field.

1 INTRODUCTION

Verification of the structural integrity of a wind turbine, according to the Draft IEC 61400-1 code [3], involves analysis of a number of fatigue load cases. The fatigue response are traditionally established using aeroelastic simulations, in which a dynamic model of the wind turbine are exposed to synthetic turbulence time series. The synthetic wind speed time series are usually generated based on knowledge to three basic turbulence characteristics - turbulence intensity, turbulence length scale and coherence.

The recommendations given in the IEC 61400-1 standard allow for two different turbulence descriptions. However, recent investigations [5] have shown that significant differences in simulated wind turbine tower fatigue loading may occur using the two suggested turbulence models. The differences in load predictions have been identified mainly to differences in the descriptions of the spatial coherence in the turbulence models.

For different terrain types, measuring levels and vertical spatial separations, the paper presents a calibration the coherence descriptions given in the existing IEC 61400-1 code for the longitudinal turbulence component.

2 THEORY

The coherence expresses the degree of agreement/correlation between (turbulence) structures, associated with two different (stationary) time series, disregarding possible phase shifts between such structures. Mathematically, the coherence is defined as normalised squared cross-spectrum amplitudes, with the normalising factors being the product of their two respective auto-spectrum amplitudes. As both the cross-spectra and the auto-spectra depend on the frequency,

the coherence will also depend on the frequency, simply meaning that the agreement between (turbulence) structures depends on their scale. The coherence takes (real) values between zero and one.

Let us consider two (turbulence) wind speed time series $u_1(t)$ and $u_2(t)$ with Fourier transforms $U_1(\omega)$ and $U_2(\omega)$, respectively. Thus

$$U_i(\omega) = \mathcal{F}[u_i(t)] ; i = 1, 2 , \quad (1)$$

where $\mathcal{F}[*]$ denotes the Fourier operator. The spectrum expresses the distribution of the energy contained in the turbulence structures on different scales. Following the definition of (one sided) spectra in [2], for sample records of length T , the auto- and cross-spectra related to the stochastic signals $u_1(t)$ and $u_2(t)$ are given by

$$S_i(\omega) = \lim_{T \rightarrow \infty} \frac{2}{T} \langle U_i(\omega) \overline{U_i(\omega)} \rangle ; i = 1, 2 , \quad (2)$$

and

$$S_{12}(\omega) = \overline{S_{21}(\omega)} = \lim_{T \rightarrow \infty} \frac{2}{T} \langle U_1(\omega) \overline{U_2(\omega)} \rangle , \quad (3)$$

respectively, where $\langle * \rangle$ denotes an ensemble averaging operator. Note, from equations (2) and (3) that the auto-spectra are real quantities, whereas the cross-spectra generally are complex.

The coherence is now expressed as

$$\gamma_{12}(\omega) = \gamma_{21}(\omega) = \frac{S_{12}(\omega) \overline{S_{12}(\omega)}}{S_1(\omega) S_2(\omega)} = \frac{S_{21}(\omega) \overline{S_{21}(\omega)}}{S_2(\omega) S_1(\omega)} , \quad (4)$$

from which it is easily seen that the coherence depends on frequency and further is a real quantity (between 0 and 1), reflecting that phase shifts have been disregarded. The coherence, as given by expression (4), refer to spectra determined from ensemble averaging. This is, however, an theoretical abstraction, and in

practice the ensemble averaging is replaced by averaging of spectra corresponding to a finite number of consecutive time samples (of equal length). The cost is that a bias is introduced in the coherence estimate. For an averaging with N statistical degrees of freedom (i.e. based on N independent time series) the *mean* estimated coherence, $E[\gamma_{12,est}(\omega)]$, relates to the true coherence as [6]

$$E[\gamma_{12,est}(\omega)] = \gamma_{12}(\omega) + \frac{(1 - \gamma_{12}(\omega))^2}{N}, \quad (5)$$

from which the true coherence is easily determined from

$$\gamma_{12}(\omega) = \frac{2 - N + \sqrt{(N-2)^2 - 4(1 - NE[\gamma_{12,est}(\omega)])}}{2}, \quad (6)$$

which especially for coherences close to zero can (depending on the magnitude of N) result in a significant correction.

Note, that in case the number of averaged elements is one (i.e. no averaging) the coherence is identical one, which can easily be verified by combining equations (3), (4) and (5).

The agreement between turbulence structures, inherent in two time series, will, apart from the frequency, also depend on the *relative* spatial position of the associated two measuring points, presuming that the turbulence field can be considered homogeneous. For inhomogeneous turbulence fields the dependence is on the *absolute* spatial position of the measuring points.

In the atmospheric boundary layer the observed spectra depend on the particular site conditions (including the thermal conditions) and the measuring height. One way to categorise *measuring site* is therefore through the integral length scale which both quantify the turbulence spectral dependence on site and thermals. The *inhomogeneous character* of turbulence in the atmospheric boundary layer is taken into account in the analysis by categorising the available measurements according to their measuring height above terrain and according to whether the measuring points are displaced vertically or horizontally.

In summary, the investigated coherences are categorised according to:

- Mean of the integral length scale associated with the two investigated turbulence time series;
- Mean of the involved measuring heights above terrain;
- Spatial displacement of the associated two measurement points; and
- Whether the measurement points are displaced vertically or horizontally.

Except for the integral length scale all the parameters defining the applied data material categories are immediately available from "Database on Wind Characteristics" [4]. The integral time scale, L_i^T , associated with the turbulence time series $u_i(t)$ is in the analysis defined as

$$L_i^T = \frac{1}{\xi^2} \int_0^T S_i \left(\frac{1}{\tau} \right) \tau d\tau ; i = 1, 2, \quad (7)$$

with

$$\xi_i^2 = \int_0^T S_i \left(\frac{1}{\tau} \right) d\tau ; i = 1, 2. \quad (8)$$

The integral length scale, L_i^L , is simple derived from the integral time scale by multiplication with the mean wind speed, \bar{u}_i , again assuming stationary processes. Thus

$$L_i^L = \bar{u}_i L_i^T ; i = 1, 2. \quad (9)$$

At a first glance, the cogent mathematical definition of the turbulence length scale as given above has the drawback that it in particular depends on the properties of the spectrum at low frequencies where the statistical significance of the spectral estimates are limited. This fact is, however, also reflected in the estimation of the coherence, where significant coherences are related to low frequencies and thereby also subjected to limited statistical significance. Thus, in this respect the present length scale definition and the coherence estimates are "consistent".

Empirical investigations show that the *coherence decay*, which is the essential/core topic for the present investigation, usually are associated with *reduced frequencies* below of the order 0.5. The reduced frequency, f_r , is defined as

$$f_r = \frac{fD}{u}, \quad (10)$$

where f is the frequency (in Hz) and D is the spatial displacement associated with the coherence parameter. The reduced frequency expresses the proportion between the spatial separation and a characteristic turbulence eddy size related to the frequency f .

The coherence is intimately related to the auto- and cross-spectral properties, and from the above discussion it is therefore obvious that the coherence decay is primary related to the spectral properties in the frequency regime $[0; f_r]$. As a consequence it is felt that, for the present purpose, the integral length scale given by equations (8), (7) and (6) is well suited as a representative (single) scale parameter for the spectral regime controlling the coherence decay.

3 DATA MATERIAL

The coherence, as described in Section 2, has been analysed based on a large number of full scale wind speed measurements extracted from "Database on Wind Characteristics" [4]. Only the horizontal turbulence component have been investigated, meaning that both cup anemometer and sonic measurements apply. However, the present investigation is solely based on cup anemometer measurements.

The sites have been selected to represent different types of terrain (flat homogeneous, coastal terrain and off-shore conditions). In the selection of sites, care have further been taken to assure that for each site category

- A large data material is available, reflecting representation of a reasonable large mean wind speed range;
- (If possible) a suitable range of vertical spacings are available, reflecting relevant wind turbine sizes;
- (If possible) at least one horizontal spacing is available.

The resulting sites with their key characteristics are specified in Table 1.

Skipheia	Hill	Coastal	H/V	5-32m/s
Cabauw	Flat	Pastoral	V	5-26m/s
Ciba	Flat	Pastoral	V	5-15m/s
Alsvik	Flat	Coastal	H	5-20m/s
Näsudden	Flat	Coastal	V	5-24m/s
Middelgrund	Flat	Off-shore	V	5-16m/s
Gedser Rev	Flat	Off-shore	V	5-16m/s
Rødsand	Flat	Off-shore	V	5-19m/s

Table 1 Site characteristics. "V" and "H" denotes that vertical and horizontal spacings are available.

Some of the selected sites offer mean wind speed values below 5m/s, however, in the present analysis only coherences associated with mean wind speeds above 5m/s are considered.

The amount of analysed data varies somewhat between the sites (Skipheia: 3290 hours; Cabauw: 473 hours; Ciba: 282 hours; Alsvik: 1740 hours; Näsudden: 2292 hours; Middelgrund: 1224 hours; Gedser Rev: 563 hours and Rødsand: 587 hours).

4 APPROACH

The present analysis is restricted to coherence behaviour in undisturbed wind fields. Therefore, measurements associated with wind turbine wake situations and measurements affected by flow distortion caused by the meteorological mast etc. have initially been discharged.

The remaining data sets have subsequently been classified according to *site*, (mean) *measuring height*, *integral length scale* and *spatial displacement* of the involved two sensors.

Basically, two different classes of spacings are considered - *vertical* spacings and *horizontal* spacings. Within each of these classes, only spacing distances of certain sizes, compared to the (mean) measuring heights, are considered. The idea behind this restriction is that the spacing distance, for a given (mean) measuring height, must correspond to a characteristic dimension of a rotor, with a hub height corresponding to the (mean) measuring height, in order to reflect the important wind turbine loadings. The following range of spacing/height ratio has (rather arbitrary) been selected

$$0.5 \leq \frac{D}{h} \leq 1.5, \quad (11)$$

where \bar{h} denotes the mean height of the relevant sensors. To address realistic wind turbine sizes, only mean measuring heights above 25m are considered.

The integral length scale classification reflects the turbulence characteristics of importance for the coherence behaviour (i.e. the terrain effect as well as the thermal impact on turbulence spectra condensed in only one descriptive parameter).

For a given "pair" of wind speed time series, belonging to an arbitrary bin class in the classification system, the data analysis is performed as follows:

- The two time series are chopped into a suitable number of segments (50% overlap have been selected) in order prepare for the spectral averaging specified in equations (2) and (3). The number of segments depends on the total length of the selected time series, and typically each segment represents a time span of the order of 5-10 minute.
- The DC component of the time segments are subtracted and the resulting time segments are detrended (linear trend assumed)
- For each segment "pair" the auto- and cross-spectra are evaluated using a FFT algorithm combined with a Hanning window, and, based on these, the average spectra are subsequently determined.
- The coherence is determined based on the averaged spectra in accordance with equation (4), and subsequently bias-corrected in accordance with equation (6). Finally, the integral length scales, associated with the two data segments, are determined based on the average spectra in accordance with equation (7) and (8), and the arithmetic mean of these are used as the length scale classification parameter for the computed coherence.

The coherence is tabulated as function of the reduced frequency defined by equation (9), and for each particular (site, height, spacing and integral length) bin class, the available coherence data are further collected in bins of the reduced frequency. The coherences belonging to each particular reduced frequency bin are finally averaged, giving the resulting coherence in terms of reduced frequency.

5 RESULTS AND DISCUSSION

The Skipheia site is outstanding both in respect to the extend of the available data material and in respect to the spatial resolution (vertical as well as horizontal) of the wind speed sensors. Therefore, the main emphasis has been put into the analysis of the data material from this site, and, as a logical consequence, the empirical coherence model to presented in Section 6 is also based on these results. The analysis of the data material from the remaining sites has primary been used to support conclusions resulting from the Skipheia analysis.

Both vertical and horizontal separation have been investigated, and in particular for the vertical separation a substantial data material is required because of an applied direction binning in the mean wind direction, which reduces the available data material substantially.

5.1 Vertical separation

For coherence analysis associated with vertical separations no direction binning is necessary, and the full data set is therefore available for the analysis. For the Skipheia site the following combinations of mean heights (h) and separations (D) have been analysed: D30h26, D31h56, D51h46, D60h71, D61h42 and D80h61. For the remaining sites, the height/separation specifications are in the same "regime" except for the Cabauw site which offers especially large mean heights and separations (D40h60, D60h50, D60h110, D100h90, D120h80, D120h140, D160h120).

Examples of measured coherences from the Skipheia site are shown in Figures 1, 2 and 3.

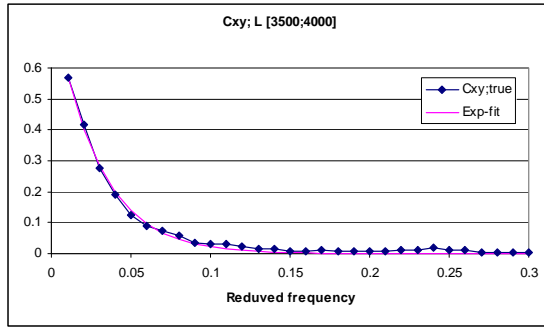


Figure 1: Coherence corresponding to a mean height equal to 26 m, a vertical spacing equal to 30 m and a length scale in the interval [3500;4000].

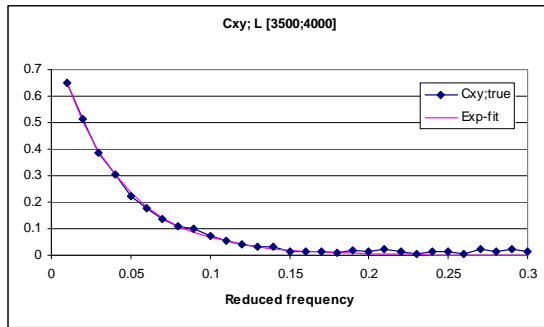


Figure 2: Coherence corresponding to a mean height equal to 56 m, a vertical spacing equal to 31 m and a length scale in the interval [3500;4000].

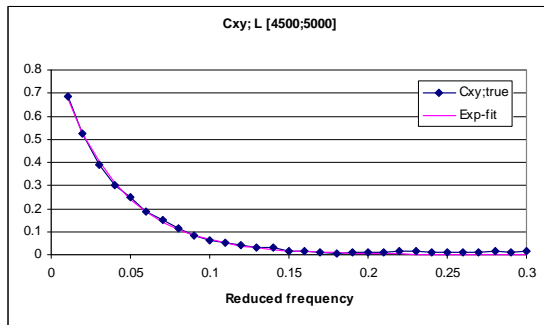


Figure 3: Coherence corresponding to a mean height equal to 56 m, a vertical spacing equal to 31 m and a length scale in the interval [4500;5000].

The following qualitative conclusions can be drawn based on the results from the analysed sites:

- The coherence increases with increasing mean height (which is also reflected comparing Figure 1 and Figure 2);
- The coherence decreases with increasing separation;

- The coherence increases with increasing length scale (which is also reflected comparing Figure 2 and Figure 3);.

The above coherence dependencies have basically the same physical background.

The dependence of the coherence with height relates to the fact that not all (large) turbulence scales are represented "close" to the surface, and that an increasing portion of these large scales tend to be represented as the measuring height is increased.

The dependence of the coherence with separation reflects that large turbulence scales are less frequent represented than smaller turbulence scales, and that coherence for large separations are associated with large turbulence scales.

The dependence of the coherence with turbulence length scale relates physically to the fact that large turbulence scales are more well represented in turbulence spectra with large length scales.

5.2 Horizontal separation

Two sites, Alsvik and Skipheia, provides possibilities for analysis of coherence associated with a horizontal separation. Unfortunately, only rather large separation distances are available (ranging between 79 m and 170 m).

Analysis of coherence associated with horizontal separation requires wind direction binning in order to assure that no (or only limited) turbulence "offset" between the relevant two sensors takes place. The direction binning is a compromise between data reduction and turbulence "offset". For the present analysis, a ± 18 deg. sector was selected corresponding to a longitudinal "offset" of the turbulence of maximal 5% of the spatial separation.

For the Skipheia site the following combinations of mean heights and separations have been analysed: D79h21, D79h41, D79h101, D170h21 and D170h41. For the Alsvik site the corresponding height/separation combinations are: D112h24, D112h31, D112h36, D112h41 and D112h53.

An example of measured horizontal coherences from the Skipheia site are shown in Figure 4.

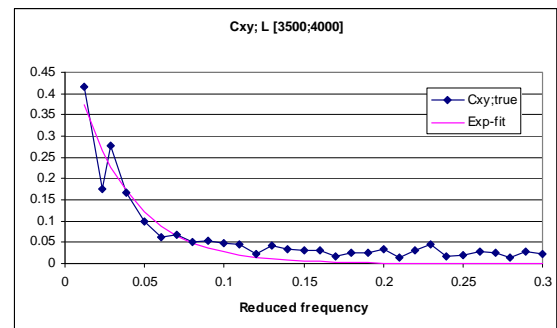


Figure 4: Coherence corresponding to a mean height equal to 41 m, a horizontal spacing equal to 79 m and a length scale in the interval [3500;4000].

As a result of the more limited data material, the coherences, corresponding to horizontal displacements, are less statistical significant than the coherences determined for the vertical displacements. The dependence of the coherence on spatial separation and

length scale seems not consistent, whereas most of the measurements display increasing coherence with increasing altitude of the sensors.

6 EMPIRICAL MODEL

The comprehensive results from analysis of the vertical coherences from the Skipheia site has been used to derive an empirical model for the coherence as function of reduced frequency, vertical separation, altitude and turbulence length scale (as defined in equation (9)).

Initially, three different types of fits were applied on the coherence data emerging from the data analysis - a traditionally 2-parameter exp-fit, a 3-parameter exp-fit and a 2-parameter sech-fit. The investigation showed that the 3-parameter exp-fit performed marginally better than the 2-parameter exp-fit, which again performed marginally better than the 2-parameter sech-fit. Based on this observation, and a wish to limit the number of model parameters as much as possible, it was decided to base the empirical model on an expression of the generic form

$$\gamma_{12}(f_r) = \text{Exp}[C_1(D, h, L^L) f_r + C_2(D, h, L^L)] , \quad (12)$$

where $C_1(D, h, L^L)$ is a *shape* parameter and $C_2(D, h, L^L)$ is a *scale* parameter. A priori it is known that both parameters must be negative in order that (12) comply with the basic features of a coherence function.

Based on the measured coherences, the shape and scale parameters are parameterised in two steps. First step relates to the turbulence length scale. Guided by the data material the following generic form of the length scale parameterisation is assumed

$$\begin{aligned} C_1(D, h, L^L) &= E_1(D, h) L^L + E_2(D, h) , \\ C_2(D, h, L^L) &= -\text{Exp}[F_1(D, h) - F_2(D, h) L^L] . \end{aligned} \quad (13)$$

Examples of the experimental results leading to the parameterisation (13) are given in Figures 5 and 6.

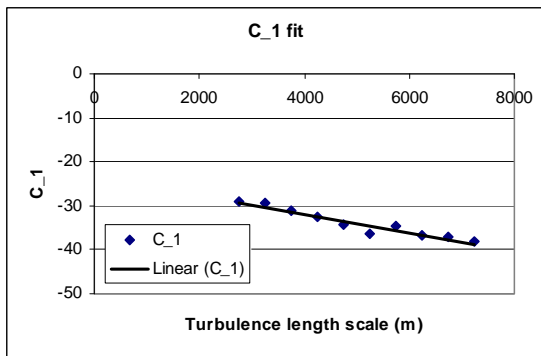


Figure 5: C_1 -parameterisation resulting from Skipheia D51h46.

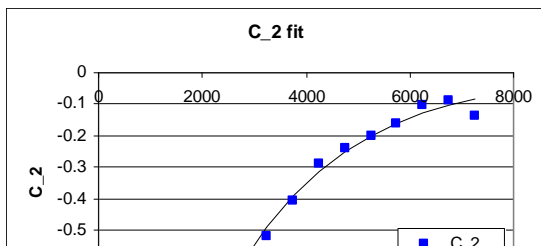


Figure 6: C_2 -parameterisation resulting from Skipheia D51h46.

The second step of the parameterisation relates to the separation and altitude parameters. Assuming that the gradients $\delta E_1/\delta D$, $\delta E_1/\delta h$, $\delta E_2/\delta D$, $\delta E_2/\delta h$, $\delta F_1/\delta D$, $\delta F_1/\delta h$, $\delta F_2/\delta D$ and $\delta F_2/\delta h$ asymptotically approach zero for D and h (individually) approaching infinity, we (otherwise rather arbitrary) assume the following generic expressions for the $E_i(D, h)$ and the $F_i(D, h)$ functions ($i = 1, 2$)

$$\begin{aligned} E_i(D, h) &= a_i D^{1/3} + b_i D^{1/3} h^{1/3} + c_i h^{1/3} + d_i + e_i D^{2/3} + f_i h^{2/3} , \\ F_i(D, h) &= \hat{a}_i D^{1/3} + \hat{b}_i D^{1/3} h^{1/3} + \hat{c}_i h^{1/3} + \hat{d}_i + \hat{e}_i D^{2/3} + \hat{f}_i h^{2/3} . \end{aligned} \quad (14)$$

The values of $E_i(D, h)$ and $F_i(D, h)$ is known in certain points (D, h) from the Skipheia results (i.e. (30,26), (31,56), (51,46), (60,71), (61,42) and (80,61)). In addition, the data material allows the gradients $\delta E_1/\delta D$, $\delta E_2/\delta D$, $\delta F_1/\delta D$ and $\delta F_2/\delta D$ to be determined for h approximately equal to 60 m (combining the D36h56 and the D80h61 results), and the gradients $\delta E_1/\delta h$, $\delta E_2/\delta h$, $\delta F_1/\delta h$ and $\delta F_2/\delta h$ to be evaluated for D approximately equal to 30 m (combining the D30h26 and the D31h56 results) and approximately equal to 60 m (combining the D61h42 and the D60h71 results).

The parameters in equation (14) are determined using a least square optimisation in which the available values of the $E_i(D, h)$ and $F_i(D, h)$ functions as well as their gradients are included. The reason for including the gradients (explicitly) are that we want to emphasise the observed coherence dependence on the altitude h and the spatial separation D . Thus the parameters in (14) are determined as the sets $(a_i, b_i, c_i, d_i, e_i, f_i)$ and $(\hat{a}_i, \hat{b}_i, \hat{c}_i, \hat{d}_i, \hat{e}_i, \hat{f}_i)$ that minimises the functionals

$$\begin{aligned} \Pi(a_i, b_i, c_i, d_i, e_i, f_i) &= \\ &\sum_{j=1}^6 [E_i(D_j, h_j) - M\{E_i(D_j, h_j)\}]^2 + \\ &\sum_{j=7}^8 \left[\frac{\partial E_i}{\partial h}(D_j, h_j) - M\left\{ \frac{\partial E_i}{\partial h}(D_j, h_j) \right\} \right]^2 + \\ &\left[\frac{\partial E_i}{\partial D}(D_9, h_9) - M\left\{ \frac{\partial E_i}{\partial D}(D_9, h_9) \right\} \right]^2 , \end{aligned} \quad (15)$$

and

$$\begin{aligned} \Theta(a_i, b_i, c_i, d_i, e_i, f_i) = & \sum_{j=1}^6 [F_i(D_j, h_j) - M\{F_i(D_j, h_j)\}]^2 + \\ & \sum_{j=7}^8 \left[\frac{\partial F_i}{\partial h}(D_j, h_j) - M\left\{ \frac{\partial F_i}{\partial h}(D_j, h_j) \right\} \right]^2 + \\ & \left[\frac{\partial F_i}{\partial D}(D_9, h_9) - M\left\{ \frac{\partial F_i}{\partial D}(D_9, h_9) \right\} \right]^2, \end{aligned} \quad (16)$$

respectively, where (D_j, h_j) , $j = 1, \dots, 9$ denotes the parameter combinations in which values of either the functions $E_i(D, h)$ and $F_i(D, h)$ or their gradients have support in the analysed coherence data. $M\{\cdot\}$ is the measurement operator giving the measured value of the argument.

The derived empirical is finally constrained to ensure that the scale parameter $C_2(D, h, L^L)$ is monotone with respect to (h, L^L) .

7 MODEL COMPARISONS

The empirical model developed (based on the Skipheia measurements) in previous section has been compared with measured coherences from *other* sites (Cabauw, Näsudden, Middelgrund, Gedser Rev and Rodsand) where it performs satisfactory, however, with a slight overestimation of the Näsudden results. The deviation between model and data in the case of Näsudden can be explained by the fact that the measured coherences for these two sites also differ, with the Skipheia coherences exceeding the Näsudden coherences.

The model has also been compared with predictions from other available models (the Mann-model [7] and the IEC-model [3]). Both the IEC-model and the Mann-model include a dependence on the turbulence length scale, however, for non of these models the length scale classification according to equation (9) has been performed. As the variation of the coherence with the length scale can be substantial, it was decided to base the comparison on data and empirical model predictions ranging from low length scales ($L^L = 2750$ m) to large length scales ($L^L = 6750$ m). The result is shown in Figure 7.

For the investigated data, the decay of the Mann coherence resembles the decay of the measured data as well as the empirical model, however with a tendency to slower decay. The decay of the IEC-model is much slower than for the measured coherences and the other two models.

The scale of the coherence depends significant on the turbulence length scale. The magnitude predicted by the IEC-model corresponds to the magnitude for measurements associated with low turbulence length scales. The magnitude predicted by the Mann-model corresponds to the measured coherences associated with large turbulence length scales.

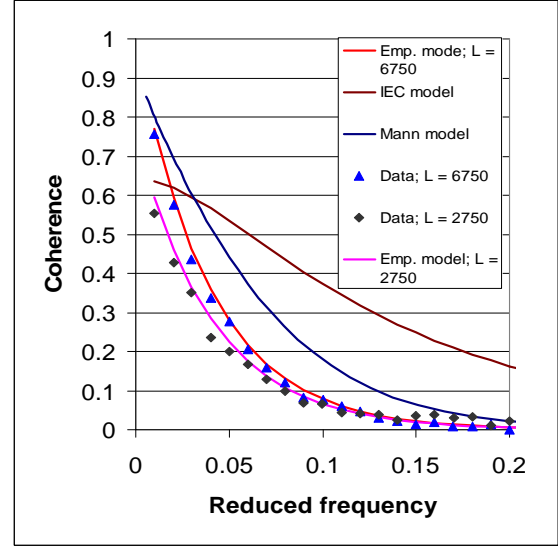


Figure 7 : Comparison of coherence predictions and measured coherences (Skipheia; D = 31m, h = 56 m).

8 CONCLUSION

An extensive amount of high sampled (horizontal) wind speed measurements from different sites have been analysed with respect to coherence behaviour. Both coherences associated with vertical and horizontal spatial separations have been investigated. However, for the coherences related to horizontal spatial separations, the data material is not consistent with respect to the dependence of the coherence with turbulent length scale and spatial separation, whereas the measured coherences clearly indicate increases levels with increasing measuring altitude and decreasing levels with increasing (reduced) frequency.

For the coherences associated with vertical separations the following qualitative conclusions can be drawn:

- The coherence decay with increasing (reduced) frequency;
- The coherence decay with increasing spatial separation;
- The coherence increase with increasing turbulence length scale; and
- The coherence increase with increasing measuring altitude.

The measured coherences associated with vertical spatial separations have been used to develop and calibrate an empirical coherence model. The empirical model has been demonstrated to fit well with the available data, however, with a slight overestimation of the Näsudden results.

The empirical model have subsequently been compared with measured coherences arising from the analysis as well as with coherences predicted by the Mann-model and the IEC-model.

Although some uncertainty exists about the turbulence length scale (in the equation (9) sense) used in the Mann and the IEC predictions, the Mann-model seems to resemble the measured data (and the predictions from new empirical model) better than the IEC-model.

ACKNOWLEDGEMENTS

The Danish Energy Agency funded the present work under the contract ENS 1363/02-0013.

Further, the analysis has benefited from measurements downloaded from the internet database: "Database of Wind Characteristics" located at DTU, Denmark. Internet: "<http://www.winddata.com/>". Wind field time series from the following sites has been applied: Cabauw (Royal Netherlands Meteorological Institute, KNMI), Näsudden and Alsvik (Dept. of Meteorology, Uppsala University), Middelgrunden, Gedser Rev, Rødsand and Ciba (Risø National Laboratories, Denmark), and Skipheia (Norwegian University of Science and Technology, Norway).

Finally, our colleague Jacob Mann is acknowledged for providing coherences predicted by the Mann turbulence model.

9 REFERENCES

- [1] Panofsky, H.A. and Dutton, J.A. (1984). Atmospheric Turbulence - Models and Methods for Engineering Applications. John Wiley & Sons.
- [2] Bendat, J.S. and Piersol, A.G. (1995). Random Data - Analysis and Measurement Procedures. John Wiley & Sons.
- [3] IEC 61400-1 Wind Turbine Safety System: part 1, Safety Requirements.
- [4] Database on Wind Characteristics.
<http://www.winddata.com/>.
- [5] Thomsen, K. (2002). The Impact of Turbulence Modelling on Tower Loads (in Danish). Risø-I-1909.
- [6] Koopmans, L.H. (1974). The Spectral Analysis of Time Series. Academic Press.
- [7] Mann, J. (1994). The Spatial structure of Neutral Surface-layer Turbulence. Journal of Fluid Mechanics, v. 273, pp. 141-168.